Cathodoluminescence of natural zircons

Cathodoluminescence of natural zircons

B Yang†, B J Luff and P D Townsend

School of Mathematical and Physical Sciences, University of Sussex, Brighton BN1 9QH, UK

Abstract. Cathodoluminescence (CL) measurements made on natural zircon crystals are reported for the temperature range 45–300 K. Different combinations of excitation conditions used at various temperatures, coupled with information on the decay lifetimes of the emission features provided by modulation of the electron beam, enable identification of excited state transitions occurring within rare-earth impurities. A broad-band feature at 385 nm is noted, in common with other luminescence studies using different forms of excitation, and is attributed to an intrinsic decay process.

1. Introduction

Zircon, $ZrSiO_4$, is a commonly occurring natural mineral with a crystal chemistry that strongly favours the incorporation of rare-earth (RE) ions as impurities. This property, coupled with the ability to form waveguides in this material by the technique of ion implantation, makes zircon of interest as a potential host material for laser waveguide cavities [1]. Spectroscopic analysis of zircon is therefore needed to identify possible laser transitions; luminescence emission has also proved useful for other optical materials as a means of providing information on sample quality. Hence, this work reports cathodoluminescence (CL) spectra from natural zircon crystals.

In most natural zircons, Dy^{3+} has been found to dominate the emission spectrum under various forms of excitation, with weaker lines often reported from Eu^{3+} and Tb^{3+}, among others (see, e.g., [2–6]). Dy^{3+} in particular is recognized as giving characteristic emission lines near 485 and 575 nm. Zircon produces particularly strong thermoluminescence (TL) signals: Kirsh and Townsend [6] analysed the kinetics and emission spectrum of the TL between 20 °C and 420 °C and support an intrinsic origin for a broad emission band at 385 nm, ascribing it to the recombination of an electron and a hole trapped at adjacent Si^{4+} and O^{2-} ions respectively, while the clear Dy^{3+} emission they observe is attributed to electron–hole recombination at the RE site.

Diaz *et al* [7] make some attempt to further unravel the emission processes occurring by comparing the spectra obtained from TL and radioluminescence (RL) studies. Measurements made with one type of excitation can provide an indirect assessment of the same features revealed using another type of excitation. The results reported in this paper therefore complement earlier data. The method used here has the advantage that information on the relative or absolute lifetimes of the various emission lines is obtained by 'chopping' the electron beam, enabling a clearer

† On leave from Beijing Normal University, Beijing 100875, People's Republic of China.

separation of the different emission processes occurring, even if they are generated at the same wavelength.

2. Experimental procedure

Measurements were made on single crystals of natural green zircon obtained from Mexico. The samples were cut and polished before examination. An electron beam of energy 2–20 keV focussed into a spot approximately 2 mm in diameter with beam currents of 0.03–4 μA was used to excite the samples. The broad diameter of the beam reduces considerably any instabilities resulting from the samples becoming charged through secondary-electron emission. Optical spectra were recorded using an $f/4$ scanning monochromator and cooled red-sensitive photomultiplier tube. The electron beam was chopped at frequencies from 5 Hz to 200 kHz and the photomultiplier output was measured on a lock-in amplifier. Measurements of the phase difference between the chopped reference signal and the output signal at various frequencies enabled decay lifetime information to be obtained. All spectral data were recorded on a computer and corrected for the spectral response of the whole detection system. The resolution was set at 5 nm. Spectra were measured in the temperature range 45 K to 300 K.

3. Results

3.1. Emission spectrum

Figure 1 shows zircon CL spectra at 300 K (*a*) and 105 K (*b*) with modulation frequencies 40 Hz and 90 Hz respectively. Twelve CL peaks with different intensities are observed at 300 K, the positions of which are at 355, 365, 385, 402, 470, 485, 530, 548, 575, 618, 670 and 760 nm. In addition, there is a broad emission band in the near-ultraviolet region, from 340 nm to 500 nm. At 105 K, three weak peaks at 460, 710 and 790 nm are recorded as well as the twelve peaks obtained at 300 K; the 355 nm peak and 548 nm peak become more intense than at room temperature and the broad band moves to 320–450 nm.
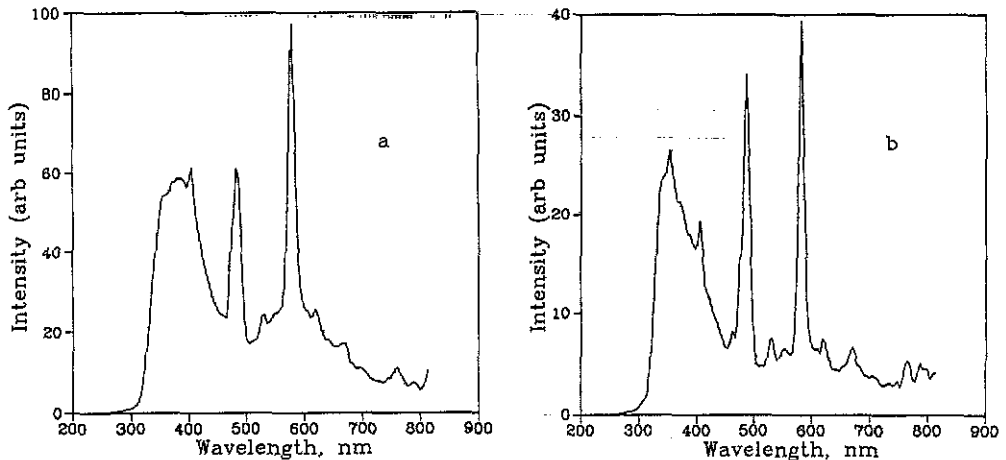

Figure 1. CL spectra of zircon at (*a*) 300 K recorded with a chopping frequency of 40 Hz and (*b*) at 105 K recorded with a chopping frequency of 90 Hz.

Changes in the relative intensities of the CL bands can be observed when different modulation frequencies are used. Spectra recorded at 300 K are shown in figure 2, with modulation frequencies 1.7 kHz and 8 kHz. Comparision with figure 1(a) shows that the 485 nm and 575 nm peaks decrease sharply as the modulation frequency increases; this is especially noticeable in the case of the 485 nm feature.
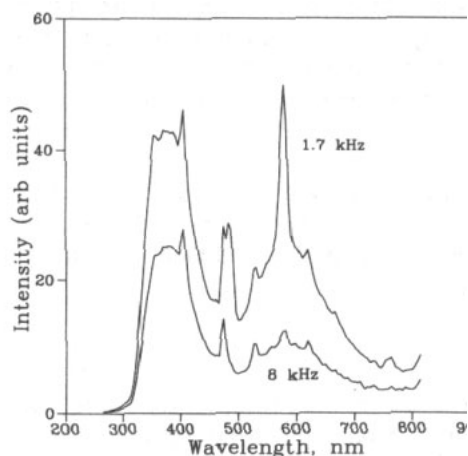

Figure 2. Zircon CL spectra at 300 K recorded at chopping frequencies of 1.7 kHz and 8 kHz.

Almost every peak has its highest intensity at about 250 K, and then decreases in intensity rapidly with decreasing temperature. Figure 3 is an isometric plot of CL intensity against wavelength and temperature; for otherwise constant excitation and recording conditions, the figure shows that there is quite a complex temperature dependence.
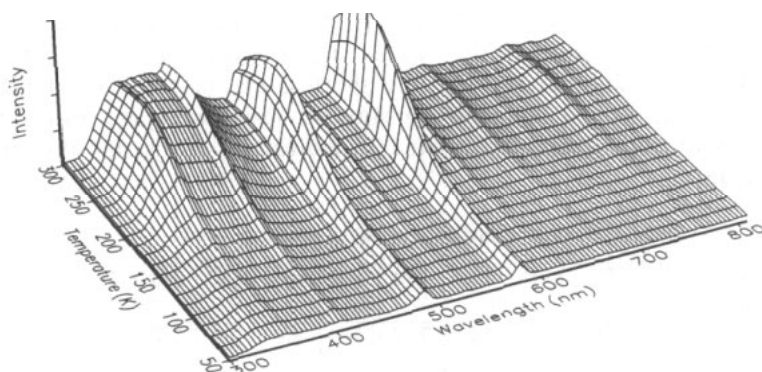
Figure 3. Isometric plot of CL intensity against wavelength and temperature.

Measurements of intensity versus irradiation dose were performed at room temperature with a 3 μA beam current, a 10 keV electron energy and 0–60 min irradiation time. As shown in figure 4, in the first 30 minutes of irradiation the intensities of the broad band and the two sharp lines at 485 nm and 575 nm are all steadily reduced, but after this time the broad band stabilizes and the two sharp lines become progressively stronger. This change is more evident for the 575 nm line, where there

is no influence from the broad band. The changes of other weaker lines cannot be measured accurately because of the overlap of the strong bands.

3.2. Lifetime

For transitions between well resolved energy states one assumes that transitions originating at a common upper level will have similar lifetimes at a chosen temperature. Lifetime data therefore should assist in assigning the upper levels of a set of transitions. More cautious consideration indicates that the transition probabilities to different lower levels are not identical since they involve the overlap of the wave-functions of the two states. Conseqently there will be perturbation caused by nearby defects and variations in lifetime with temperature.

It is evident from the reaction of different lines to various modulation frequencies that the zircon emission bands possess quite different lifetimes. However, absolute measurement of the lifetimes of individual lines was found to be difficult because of the effects of overlapping bands having similar lifetimes. The relation

$$\tan \Delta\phi = 2\pi f \tau$$

(see Demtroder [8]), where $\Delta\phi$ is the measured phase difference between reference and signal at frequency f and τ is the lifetime, is not applicable when the decay is non-exponential in character, e.g. when more than one exponentially decaying feature contributes to the measured signal. Graphs of the measured phase shifts against frequency for the various line features indicated that the decays were non-exponential in most cases; the lifetimes of the twelve peaks given in table 1 at 45, 250 and 300 K are therefore to be considered only as estimates of the absolute lifetimes. The main information is obtained from the relative values of the numbers given, which were calculated using the above equation by varying the modulation frequency to produce the same phase shift for each line, thus revealing differences in decay characteristics between the various lines. The data in table 1 show that the twelve peaks can be roughly grouped into three sets. The set consisting of the 485 nm and 575 nm bands possesses the longest lifetime; the four bands with the shortest wavelengths form another set with the shortest lifetimes and the third set includes all the other bands. The bands in the same set may have some common luminescent process since lifetime may be related to activation energy for thermal detrapping processes [6].

Table 1. Estimated lifetimes of zircon emission bands.

Wavelength (nm)		355	365	385	402	470	485	530	548	575	618	670	760
Lifetime $(10^{-5}s)$	45 K	0.59	0.45	0.45	0.53	5.4	9.0	7.3	7.7	9.1	5.0	7.2	7.4
	250 K	0.51	0.45	0.43	0.53	6.8	19.0	5.6	5.6	15.9	5.8	6.3	8.9
	300 K	0.39	0.39	0.29	0.41	3.6	4.8	3.6	4.7	3.3	3.8	3.4	5.2

A strong temperature dependance of the measured lifetime of every band is obtained. The lifetime of every band reaches a peak value at about 250 K; figure 5 shows the lifetimes of emission recorded at 402, 485 and 618 nm as a function of temperature.
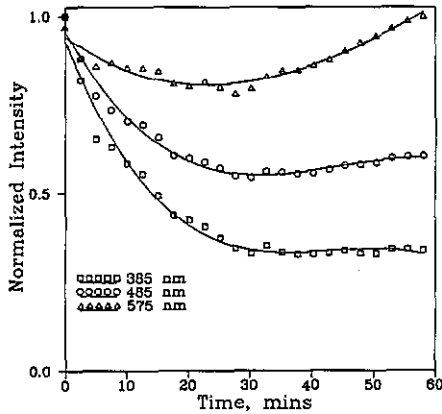
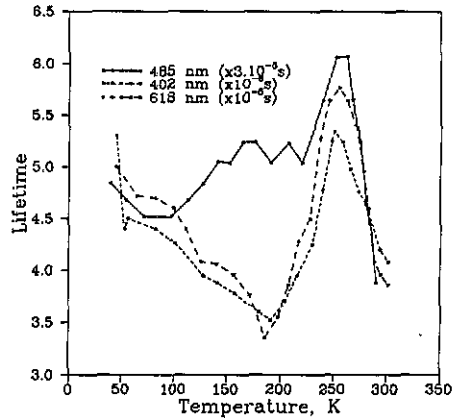**Figure 4.** Normalized CL intensity plotted against irradiation time for emission at 385, 485 and 575 nm.

Figure 5. Lifetimes of the 402, 485 and 618 nm bands as a function of temperature.

4. Discussion

Many of the cathodoluminescence bands detected in this work are also found in the TL spectra of zircon [6]. Following the discussion in [6], the emission bands of zircon can be classified as intrinsic emission and impurity luminescence. Those sharp lines with wavelengths longer than 450 nm are from the naturally present RE impurities, such as Dy^{3+}, Tb^{3+}, and the broad band below 450 nm is an overlap of a broad intrinsic band and some RE^{3+} sharp lines.

The following explanation for the occurrence of the intrinsic broad band was given by Iacconi *et al* [5] in their report on the TL spectra of zircon x-ray irradiated at 77 K: free electrons and holes are produced by the irradiation and some of them are trapped on Si^{4+} and adjacent O^{2-} ions respectively. When the crystal is later heated up, electrons are thermally released and recombination occurs, accompanied by the emission of photons. Kirsh and Townsend [6] showed that this model can also explain the TL spectra at above room temperature. In the present work the broad band in the CL spectra can be explained with the same model, except that the recombination electrons are not thermally released but are released from Si^{3+} ions by the incident high-energy electron beam. Different activation energies are needed for the reaction described above, as the separations of the Si–O pairs between which the recombinations occur may be different. By contrast with TL, excitation by the high-energy electron beam excites all possible kinds of recombination; this leads to the lifetime of the broad band being a complicated function of temperature. The high collision densities may even stimulate some processes that are negligible for the low dose rates of RL.

Dy^{3+} and Tb^{3+} are common impurities of natural and undoped artificial zircon crystals. As for those in the TL spectrum, the sharp lines in the CL spectrum of zircon result from transitions between Dy^{3+} and Tb^{3+} energy levels. The energy level diagrams for these two ions in $LaCl_3$ as determined by Dieke and Crosswhite [9] are shown in figure 6; the labelling of the levels with no *LSJ* term are as given in this reference. The observed CL emission bands were related to specific transitions

and the resulting energy level assignments are shown in tables 2 and 3. Some of our conclusions are different from those suggested in [6], but it should be noted that the TL and RL data in that reference were obtained with a lower wavelength resolution than used for this CL study.

Figure 6. Energy levels of Dy^{3+} and Tb^{3+}.

The suggested assignments given in tables 2 and 3 are supported by the lifetime measurements. As outlined in the above section, it is suggested by the data in table 1 that the two strong sharp lines at 485 and 575 nm belong to the same set, and table 2 shows that they have the same initial excited state, i.e. $^4F_{9/2}$ of Dy^{3+} (figure 6). State I of Dy^{3+} is the initial excited state of almost all the weaker lines grouped in another set by the lifetime measurement. The broad intrinsic near-ultraviolet emission band possesses the shortest lifetime given in table 1; the lifetimes of the overlapping RE^{3+} lines in this region cannot be measured because they cannot be separated from this much stronger feature. Figure 6 also shows transitions from the $^5D_4$ level of Tb^{3+}; the luminescence bands arising from these transitions all have similar lifetimes.

Table 2. Suggested transitions between Dy^{3+} levels.

Wavelength (nm)	402		460		470	485	530	548	575	618		670		710		760	790
Energy (eV)	3.08		2.70		2.64	2.56	2.34	2.26	2.16	2.01		1.86		1.74		1.63	1.57
Dy^{3+} i	T	I	O	L	I	$^4F_{9/2}$	I	L	$^4F_{9/2}$	I	I	$^4F_{9/2}$	I	L	I	$^4F_{9/2}$	I
f	$^6F_{1/2}$ $^6H_{5/2}$	$^6H_{7/2}$	$^6F_{11/2}$ $^6H_{9/2}$	$^6H_{9/2}$	$^6H_{11/2}$	$^6H_{11/2}$	$^6H_{9/2}$	$^6F_{9/2}$ $^6H_{7/2}$	$^6H_{11/2}$	$^6F_{9/2}$ $^6H_{9/2}$	$^6F_{9/2}$ $^6H_{7/2}$	$^6H_{11/2}$	$^6H_{9/2}$	$^6F_{9/2}$	$^6F_{9/2}$	$^6F_{9/2}$ $^6H_{7/2}$	$^6F_{9/2}$

The fact, shown in figure 2, that under the higher modulation frequencies the 575 nm peak decreases less than the 485 nm peak indicates that we may not be resolving two closely similar transitions. That is, the initial state of the measured 575 nm line is not only the Dy^{3+} $^4F_{9/2}$ state but also the state labelled I, and similarly the more evident decrease of the 670 nm line compared with the other weaker lines also indicates that two excited states, i.e. levels $^4F_{9/2}$ and I of Dy^{3+}, are involved (table 2).

Those peaks that can only be clearly recorded at low temperature, i.e. 338, 460, 548, 710 and 790 nm, may be from higher excited states. These states are very close to the conduction band, so they are stable only at low temperature. This is consistent with the results given in table 2.

Table 3. Suggested transitions between Tb^{3+} levels.

Wavelength (nm)		355	365	385	460	470	485	548	618	670
Energy (eV)		3.50	3.40	3.22	2.70	2.64	2.56	2.26	2.01	1.86
Tb^{3+}	i	K	K	$^5D_3$	$^5D_3$	$^5D_3$	$^5D_3$	$^5D_4$	$^5D_4$	$^5D_4$
	f	$^7F_2$	$^7F_0$	$^7F_6$	$^7F_3$	$^7F_2$	$^7F_0$	$^7F_5$	$^7F_3$	$^7F_1$

It is difficult to determine the origins of the 760 nm and 790 nm bands. The measurement of energy difference from figure 6 shows that the 760 nm line transition occurs between the Dy^{3+} levels $^4F_{9/2}$ and $^6F_{9/2}$ or $^6H_{9/2}$, but its lifetime is obviously shorter than the other two transitions from the $^4F_{9/2}$ state. The 790 nm line appears only at low temperature, but no relative high initial excited level can be found for it. Further investigations are almost impossible for these two weak lines.

RE^{3+} ions substitute for Si^{4+} ions in zircon and normally charge compensation is required. Some of the RE^{3+} ions reduce during the irradiation to RE^{2+} by capturing electrons. The holes produced by this process are trapped in various types of hole trap. Trapped holes can be released by later excitation. RE^{3+} ions in excited states are produced by the recombination of the released holes and electrons of RE^{2+} ions.

The energy to release the trapped holes comes from the incident electrons and also possibly from the ultraviolet photons emitted by SiO_4 clusters mentioned above. In the measurement of emission intensities versus irradiation dose, we find that the RE^{3+} peaks start increasing in intensity when the near-ultraviolet broad band stops its fast decrease (figure 4). This implies that there may be some close relation between these two different emissions.

Although it is difficult to give detailed models for the hole traps, we may speculate that they are neighbouring O^{2-} ions, or some other related structures. Nevertheless, it is certain that the recombination is not only one simple process, but a mixture of several complicated processes. This complication is demonstrated by the relations between the lifetimes and temperature for the RE^{3+} lines shown in figure 5.

5. Conclusions

Tables 2 and 3 summarize the suggested assignments of transition levels for the main sharp emission lines found in this study. Nearly all are attributed to the RE elements

Dy^{3+} and Tb^{3+}. Separation of the various lines by decay lifetime has enabled a more positive grouping of the lines into transitions occurring from particular initial states, demonstrating the value of the pulsed excitation technique. As distinct from earlier data, the lifetime measurements reveal that some lines were insufficently resolved and contributions from similarly spaced transitions can occur (e.g. near 460, 575, 670 and 710 nm). An intrinsic feature at 385 nm, also found in other luminescence studies using different types of excitation and attributed to recombination of electrons released from Si^{4+} sites at O^{2-} sites, has a complex temperature behaviour. This complexity is explained by the different activation energies associated with recombination between Si-O atoms having different atomic separations; if the electron beam is assumed to itself provide the energy needed for the transition (as opposed to, say, a thermally activated process) then a combination of all possible transitions might be expected to be occurring at the same time.

Acknowledgments

References

[1]   Babsail L, Hamelin N and Townsend P D 1991 *Nucl. Instrum. Methods Phys. Res.* **B59/60** 1219
[2]   Chee J, Oczkowski H L, Kirsh Y, Scott A, Siyanbola W G and Townsend P D 1988 *Nucl. Tracks Radiat. Meas.* **14** 35
[3]   Templer R H 1986 *DPhil Thesis* University of Oxford
[4]   Godfrey-Smith D I, McMullan W G, Huntley D J and Thewalt M L W 1989 *J. Lumin.* **44** 47
[5]   Iacconi P, Lapraz D, Barthe J, Keller P, Portal G 1980 *Phys. Status Solidi* a **59** 639
[6]   Kirsh Y and Townsend P D 1987 *J. Phys. C: Solid State Phys.* **20** 967
[7]   Diaz M, Luff B J, Townsend P D and Wirth K R 1991 *Nucl. Tracks Radiat. Meas.* **18** 45
[8]   Demtroder M 1981 *Laser Spectroscopy* (Berlin: Springer) p 557
[9]   Dieke G H 1968 *Spectra and Energy Levels of Rare Earth Ions in Crystals* (New York: Wiley)